THE ASTROPHYSICAL JOURNAL, 473:304–309, 1996 December 10

A NEW LOOK AT CARBON ABUNDANCES IN PLANETARY NEBULAE. II. BB 1, NGC 650, NGC 1535, NGC 2440, AND NGC 7027

K. B. KWITTER
Department of Astronomy, Williams College, Williamstown, MA 01267; Karen.B.Kwitter@williams.edu
AND
R. B. C. HENRY
Department of Physics and Astronomy, University of Oklahoma, Norman, OK 73019; henry@phyast.nhn.uoknor.edu
Received 1996 March 22; accepted 1996 July 8

ABSTRACT

This paper is the second in a series that reports on the outcome of a study of carbon abundances in a carefully chosen sample of planetary nebulae representing a large range in progenitor mass and metallicity. We use the Final Archive *IUE* database containing consistently reduced *IUE* spectra to measure line strengths of C III] λ1909, along with numerous other UV lines for the planetary nebulae BB 1, NGC 650, NGC 1535, NGC 2440, and NGC 7027. Combining these measurements with optical data from the literature, we determine values for the abundance ratios He/H, O/H, C/O, N/O, and Ne/O for these five objects using a five-level program, but we fine-tune the results with corrections derived from detailed photoionization models constrained by the same set of emission lines. All five objects show enhanced levels of C/O and N/O but depleted O/H with respect to the Sun.

Subject headings: ISM: abundances — planetary nebulae: general — stars: evolution — ultraviolet: ISM

1. INTRODUCTION

We are involved in a project the purpose of which is to determine the stellar yield of carbon as a function of stellar mass and metallicity for intermediate-mass stars. These objects span the mass range $0.8 < M < 8\ M_{\odot}$ and are predicted to produce as much as 60%–80% of the carbon in the Galaxy. We are measuring *IUE* spectra of planetary nebulae (PNs) containing strong, collisionally excited carbon emission lines: spectra that have been rereduced in a systematic way (Final Archive). These data are then joined with published optical data; subsequently, five-level atom and photoionization model calculations are used to determine the abundance ratio of C/O, in particular, but also He/H, O/H, N/O, and Ne/O for a select sample of 22 planetary nebulae that were chosen to represent a broad range in progenitor mass and metallicity. Ultimately, we will use our abundance results as constraints for our own stellar evolution models in order to derive the stellar yield of carbon as a function of these two parameters.

In our first paper (Henry, Kwitter, & Howard 1996, hereafter Paper I), we listed our sample objects, described our project in detail, and presented results for four PNs: PB 6, Hu 2-1, K648, and H4-1. In this paper, we describe our analysis of five additional PNs: BB 1, NGC 650, NGC 1535, NGC 2440, and NGC 7027. Subsequent papers will report on the remaining 13 objects, as well as present and discuss stellar model predictions of carbon yields for intermediate-mass stars.

Section 2 describes the data used in the analysis of these five objects. The abundance calculations and results are presented in § 3, and a summary is contained in § 4. More detailed discussion of the project and procedures may be found in Paper I.

2. THE DATA

We employed short-wavelength prime (SWP) spectra from the Final Archive of *IUE*. These spectra have recently been systematically and uniformly rereduced by *IUE* staff using state-of-the-art procedures unavailable at the time the spectra were observed.

In Paper I, we deliberately chose PNs of relatively small angular size that fit entirely within both the large *IUE* aperture (21.″7 × 9.″1) as well as the slits that were used to obtain the optical spectra taken from the literature and to compute abundance ratios as described above. Beginning with this paper, we analyze several objects that are larger than the smallest dimension of the *IUE* slit; thus, care must be taken to choose optical data that match as closely as possible the region of the nebula observed with the *IUE*. Only one of the five objects presented here (BB 1) was small enough to fit within both the *IUE* and optical slits. Nevertheless, in the remaining four cases we were able to couple *IUE* and optical data that shared some overlap. Thus, we feel that the abundances derived from the spectral coupling provide reasonable estimates of all ratios for each PN.

Table 1 lists the archived spectra that were measured for each of the five program objects considered here. Also shown are the integration times. In all cases, the size of the *IUE* slit was 21.″7 × 9.″1. When more than one spectrum was available for the same location, our adopted line strengths represent averages weighted appropriately by integration time. From the numerous sources of optical line strengths for each of our objects in the literature, we attempted to choose the set that best matched the *IUE* data in terms of the nebular region observed—i.e., position with respect to the central star and position angle. We now provide some detailed comparison by object of the optical and *IUE* observations with regard to positions.

BB 1.—We used optical observations from Torres-Peimbert, Rayo, & Peimbert (1981), who employed a 3.″8 × 12.″4 rectangular slit oriented east-west. With an optical diameter of 3″ (Acker et al. 1992), light from this object fell entirely within both the optical and *IUE* slits, and therefore positional overlap was moot.

NGC 650.—Optical line strengths of Peimbert & Torres-Peimbert (1987) were adopted where their slit was 3.″8 × 12.″4 oriented east-west and centered on the bright nebu-

TABLE 1

FINAL ARCHIVE SPECTRA

SWP	Exposure Time (s)
BB 1	
45331.....	1500
45332.....	1500
45338.....	1500
45339.....	1500
45340.....	1800
45341.....	1800
45345.....	3600
45346.....	1200
45347.....	1200
45368.....	1500
NGC 650	
38257.....	14400
NGC 1535	
15497.....	3000
NGC 2440	
5235	1800
5236	360
NGC 7027	
1913	720
1914	2160
2430	1800
3202	720
6542	3600
17241.....	720
17242.....	10800

losity at 34.″7 west and 26.″0 south. The *IUE* slit was centered on the same location but with a position angle of 302°. Thus, we judge our positional overlap for this object to be quite good, although not exact.

NGC 1535.—The optical line strengths of Gutiérrez-Moreno, Moreno, & Cortés (1985) were employed for this object. They used a 36.″4 diameter circular aperture, which essentially captured light from the entire 21″ nebula (Acker et al. 1992). The *IUE* aperture was centered at a point 8″ north of the central star at a position angle of 229°. Again, overlap is good.

NGC 2440.—Line strengths from Shields et al. (1981) were used. They employed a 10″ × 20″ elliptical slit that was oriented at a position angle of 10° and centered on the central star. The *IUE* spectra were also centered on the central star with a position angle of 10°. With an optical diameter of 16″ for NGC 2440 (Acker et al. 1992), positional overlap is reasonably good.

NGC 7027.—We employed the mean optical line strengths of Kaler et al. (1976), which represent data from different locations averaged together. Each of the seven *IUE* spectra was taken with a different position angle; thus, we average these to obtain a spectrum representative of the entire nebula. We judge the overlap to be very good.

Ultraviolet line strengths of C III] λ1909, C IV λ1549, and other lines of interest to this program were measured with routines in IRAF.[1] Fluxes uncorrected for reddening are presented in Table 2, columns (3), (5), (7), (9), and (11), where these flux values have been normalized to Hβ = 100 using the observed value of $F_{H\beta}$ shown in the third row from the bottom of the table. These line strengths in turn were corrected for reddening by assuming that the relative strength of Hα/Hβ = 2.86, computing the logarithmic extinction quantity c shown in the table, and adopting Seaton's (1979) extinction curve for the UV lines. Values for the reddening coefficients are listed in column (2). A final adjustment was carried out by scaling the UV lines so that the line strength ratio of the He II lines $\lambda\lambda$1640/4686 was equal to the value given in the bottom row of the table. These values were determined using electron temperature and density information from the optical spectra along with results in Hummer & Storey (1987). Columns (4), (6), (8), (10), and (12) list our final, corrected line strengths, again normalized to Hβ = 100. Uncertainties (shown in parentheses) were determined using the scheme described in Paper I. Finally, optical information for each object—including information on $F_{H\beta}$, the Balmer decrement, He II λ4686, and all optical lines used to infer abundance ratios—were taken from the references given in the footnotes of Table 2. Where possible, we began with observed fluxes and corrected them for extinction using the reddening curve of Savage & Mathis (1979). In cases where only dereddened intensities were reported, we reversed the authors' dereddening procedure in order to extract their observed fluxes, then we applied the Savage & Mathis curve to obtain a new version of intensities consistent with the others.

3. RESULTS

3.1. *Abundance Calculations*

Abundance calculations for the ratios He/H, O/H, C/O, N/O, and Ne/O were carried out following the steps given in detail in Paper I. In brief, we take a set of merged UV and optical line strengths for each PN and use the five-level atom routine "ABUN" to derive an initial set of abundance ratios $A^{PN}_{ABUN}(X)$, where X is one of the five abundance ratios listed above. Using the program CLOUDY (Ferland 1990), we then calculate a photoionization model for each object, in which we match a set of five diagnostic ratios formed from specific observed intensities: $(I_{[O\,II]} + I_{[O\,III]})/I_{H\beta}$, $I_{[O\,II]}/I_{[O\,III]}$, $I_{He\,II/He\,I}$, $I_{\lambda4363/\lambda5007}$, and $I_{\lambda6716/\lambda6731}$.[2] The first ratio provides a constraint on nebular metallicity and stellar temperature, the second and third ratios constrain the ionization parameter and stellar temperature, and the fourth and fifth ratios constrain electron temperature and density, respectively. (Note that since Paper I we have included the helium line strength ratio as an additional constraint.) Now taking the set of predicted line strengths from the model output, we use "ABUN" to derive "observed" abundance ratios $A^{mod}_{ABUN}(X)$ for the model and compare these with the actual model input abundance ratios $A^{mod}_{in}(X)$. Then we arrive at our final set of abundance

[1] IRAF is distributed by the National Optical Astronomy Observatories, which is operated by the Association of Universities for Research in Astronomy, Inc. (AURA), under cooperative agreement with the National Science Foundation.

[2] I refers to line intensities. [O II] and [O III] mean λ3727 and $\lambda\lambda$4959, 5007, respectively. He II and He I refer to the lines λ4686 and λ5876, respectively. The final two line ratios involve the auroral and nebular lines of [O III] and the [S II] doublet density diagnostic.

1996ApJ...473..304K

TABLE 2

UV LINE STRENGTHS[a]

		BB 1[b]		NGC 650[c]		NGC 1535[d]		NGC 2440[e]		NGC 7027[f]	
LINE (1)	$f(\lambda)$ (2)	$F(\lambda)$ (3)	$I(\lambda)$ (4)	$F(\lambda)$ (5)	$I(\lambda)$ (6)	$F(\lambda)$ (7)	$I(\lambda)$ (8)	$F(\lambda)$ (9)	$I(\lambda)$ (10)	$F(\lambda)$ (11)	$I(\lambda)$ (12)
C III λ1175	1.85	...	...	...	...	5(±1)	26(±2)	...	...	...	...
N V λ1240	1.64	93(±92)	100(±121)	...	...	3(±1)	17(±1)	11(±2)	120(±26)	0.1(±0.04)	26(±9)
C II λ1336	1.41	68(±34)	69(±53)	3(±2)	14(±11)	...	...	...	...	...	...
O IV] λ1404	1.30	...	...	13(±4)	53(±32)	...	...	8(±2)	59(±15)	1(±0.2)	63(±19)
N IV] λ1485	1.23	48(±25)	46(±33)	...	...	...	...	34(±5)	218(±37)	0.7(±0.12)	52(±10)
C IV λ1549	1.18	1434(±217)	1355(±701)	...	...	13(±2)	68(±3)	80(±12)	483(±82)	20(±3)	1306(±222)
[Ne V] λ1575	1.17	77(±48)	73(±57)	...	...	1(±0.4)	4(±1)	2(±1)	10(±6)	...	...
[Ne IV] λ1602.....	1.15	...	...	...	...	...	...	...	...	0.2(±0.05)	13(±3)
He II λ1640.....	1.14	181(±33)	169(±86)	74(±16)	265(±137)	16(±2)	82(±3)	73(±11)	408(±71)	5(±0.1)	313(±24)
O III] λ1660	1.13	82(±39)	76(±51)	...	...	2(±0.6)	10(±1)	8(±2)	43(±12)	0.9(±0.2)	49(±12)
Si II λ1711	1.12	...	...	...	...	0.1(±0.05)	0.4(±0.1)	2(±1)	8(±6)	...	...
N III] λ1750	1.12	27(±9)	25(±14)	30(±11)	106(±62)	1(±0.6)	5(±1)	29(±4)	160(±26)	0.6(±0.1)	32(±6)
C II] λ1760	1.12	...	...	...	...	0.2(±0.1)	0.8(±0.1)	...	...	...	...
Si II λ1808	1.14	...	...	...	...	...	...	0.5(±0.2)	3(±1)	...	...
C III] λ1909	1.23	1180(±175)	1130(±606)	322(±48)	1250(±658)	27(±4)	139(±5)	141(±21)	892(±155)	14(±2)	1062(±172)
log $F_{H\beta}$[g].....		−12.47(±0.06)	...	−12.43(±0.06)	...	−10.45(±0.01)	...	−10.50(±0.01)	...	−10.12(±0.01)	...
c		...	0.12(±0.18)	...	0.35(±0.18)	...	0.07(±0.03)	...	0.57(±0.03)	...	1.10(±0.03)
λ1640/λ4686[h].....		...	6.71	...	6.71	...	6.38	...	6.90	...	6.93

[a] Normalized to Hβ = 100.
[b] Optical information taken from Torres-Peimbert et al. 1981.
[c] Optical information taken from Peimbert & Torres-Peimbert 1987.
[d] Optical information taken from Gutiérrez-Moreno et al. 1985.
[e] Optical information taken from Torres-Peimbert & Peimbert 1977 and Shields et al. 1981.
[f] Optical information taken from Shaw & Kaler 1982 and Kaler et al. 1976.
[g] In units of ergs cm^{-2} s^{-1}.
[h] Ratio of He II lines used to merge UV and optical line strengths. Data taken from Hummer & Storey 1987.

TABLE 3A

OBSERVATIONS AND MODELS[a]

PARAMETER	BB 1		NGC 650		NGC 1535		NGC 2440		NGC 7027	
	Observation	Model	Observation	Model	Observation	Model	Observation	Model	Observation	Model[b]
$\log(I_{[O\,II]} + I_{[O\,III]})/H\beta$	+0.69	+0.82	+1.35	+1.40	+1.23	+1.24	+1.33	+1.34	+1.28	+1.29
$\log I_{[O\,II]} + I_{[O\,III]}$	−1.65	−1.81	−0.43	−0.47	−2.21	−2.15	−1.17	−1.20	−1.88	−1.82
$\log I_{He\,II/He\,I}$	+0.39	+0.25	+0.49	+0.54	+0.04	−1.40	+0.87	+0.76	+0.60	+0.71
$\log I_{\lambda 4363}/I_{\lambda 5007}$	−1.94	−1.84	−1.95	−1.98	−1.96	−1.75	−1.77	−1.76	−1.75	−1.69
$\log I_{\lambda 6716}/I_{\lambda 6731}$	...	−0.11	+0.06	+0.08	...	−0.31	−0.21	−0.20	−0.35	−0.35
T_{eff} (10^3 K)	...	125	...	220	...	50	...	200	...	170
$\log U$	...	−1.10	...	−3.00	...	−0.50	...	−2.20	...	...
N_e	...	1700	...	400	...	17000	...	5700	...	...
[He/H]	...	0.00	...	+0.15	...	−0.05	...	+0.04	...	+0.01
[O/H]	...	−0.92	...	−0.10	...	−0.70	...	−0.23	...	−0.07
[C/O]	...	+1.60	...	+0.85	...	−0.06	...	+0.41	...	+0.98
[N/O]	...	+1.04	...	+0.48	...	−0.26	...	1.15	...	+0.32
[Ne/O]	...	0.80	...	+0.30	...	+0.01	...	−0.01	...	+0.33
[S/O]	...	−0.52	..	−0.10	...	+0.00	...	−1.70	...	+0.09

[a] Model input abundances are expressed logarithmically and normalized to solar values.

[b] Output and input for model F1 from Péquignot et al. 1978 was used in our analysis of NGC 7027. They used a model atmosphere of $T_{eff} = 1.7 \times 10^5$ K for the central ionizing source along with a two-component nebula, where the components had densities of 2.5×10^5 cm^{-3} and 6.0×10^4 cm^{-3}. U parameter considerations are of little value in this case, so no value is given.

ratios $A_F^{PN}(X)$ for the PN under investigation by assuming that

$$A_F^{PN}(X) = A_{abun}^{PN}(X)\xi(X)\,, \tag{1a}$$

where

$$\xi(X) = \frac{A_{in}^{mod}(X)}{A_{abun}^{mod}(X)}\,. \tag{1b}$$

Note in equation (1a) that we are applying the correction factor ξ to the preliminary abundances A_{abun}^{PN} derived directly from the observed line strengths and not the model input abundances given in Table 3A. Rather, the latter abundance sets are provided only for the sake of completeness.

Our modeling results are summarized in Table 3A, where for each PN we list the observed and model-predicted diagnostic line ratios in the first five rows. Below this information are listed the model input parameters for the best model. Note that for NGC 7027, rather than calculating our own model, we have adopted model F1 of Péquignot, Aldrovandi, & Stasińska (1978), since their model achieved an excellent match with the observed line strengths from Kaler et al. (1976). As a comparison exercise, stellar temperatures and nebular electron densities that were used in each of our best-fit models are presented in Table 3B along with analogous values from other sources.

Notice that in Table 3A, the observed and modeled ratios agree to within roughly 0.15 dex in all but $I_{He\,II/He\,I}$ in NGC 1535. Information in Table 3B indicates that, likewise, our model effective temperatures and electron densities are consistent with other values found in the literature, except for our inferred electron density for NGC 1535. Apparently, NGC 1535 is a trouble spot.

NGC 1535 was also modeled by Adam & Köppen (1985), who invoked a complex ionizing source comprising a non-LTE stellar atmosphere and a hot circumstellar gas to

TABLE 3B

COMPARISON OF CENTRAL STAR TEMPERATURES AND NEBULAR DENSITIES

PARAMETER	BB 1		NGC 650		NGC 1535		NGC 2440	
	Current	P	Current	K	Current	A, G	Current	S
$T_*(10^3$ K)	125	...	220	162	50	50	200	166
$N_e(10^3$ cm^{-3})	1.7	3.0	0.4	0.3	17.0	6.0	5.7	4.0

SOURCES.—P = Peña et al. 1991; K = Kaler, Shaw, & Kwitter 1990; A = Adam & Köppen 1985; G = Gutiérrez-Moreno, Moreno, & Cortés 1986; S = Shields et al. 1981.

TABLE 3C

CORRECTION FACTORS (ξ)

Ratio	BB 1	NGC 650	NGC 1535	NGC 2440	NGC 7027
He/H	1.03	0.97	1.00	1.16	1.06
O/H	1.05	0.99	0.98	1.15	1.28
C/O	2.33	0.94	1.64	1.02	1.59
N/O	1.00	0.85	0.95	1.01	0.99
Ne/O	0.89	0.68	0.90	0.95	2.47

produce adequate amounts of photons with energies above 54 eV to match the strong observed He II λ4686 line strengths. They offer two best-fit models: one is optically thin and the other is optically thick, and both do a satisfactory job of matching four of five of our diagnostic ratios—i.e., their helium ratio matches the observed ratio, but they have difficulty reproducing the observed [O II]/[O III] ratio. NGC 1535 is apparently a complicated object, which to this point appears to be model intractable. It is also not possible at present to resolve the discrepancy regarding our electron density and values in the literature because the lines [S II] λλ6716, 6731 are too weak to measure (Torres-Peimbert & Peimbert 1977); instead, the density estimates have been derived using diagnostic diagrams. Through our modeling we derive an electron density roughly 3 times greater than inferred previously.

Finally, Table 3C lists the correction factors ξ. A value of unity represents complete consistency between abundance ratios derived using output emission lines and input abundances in the models. Clearly, ξ is a model-determined gauge of how closely the abundances derived with our five-level atom program agree with the actual nebular abundances.

3.2. *Derived Abundances*

Our final abundances for the five PNs being studied here are presented in Table 4 and Figure 1. In the table, the first column shows the ratios of interest, and the remaining columns report our derived abundance ratios. Listed beneath each abundance ratio is our estimate of percent uncertainty for that ratio. These values are based only upon uncertainties in line strength considerations and do not include any assessment of systematic errors inherent in our method for determining abundances. The last column contains solar values for the corresponding ratios taken from Grevesse & Anders (1989) for comparison, and the bottom row lists the Peimbert class of each of our objects. Figure 1 shows graphically our derived abundance ratios. Ratios derived here are shown with filled symbols, with symbol shape representing specific objects as defined in the figure legend. Error bars show the uncertainties given in Table 4. For comparison, abundance ratios taken from the literature are shown with open symbols. In this case, all abundance information for BB 1 was taken from Peña, Torres-Peimbert, & Ruiz (1991). For the remaining four objects, all C/O ratios came from Rola & Stasińska (1994), while values

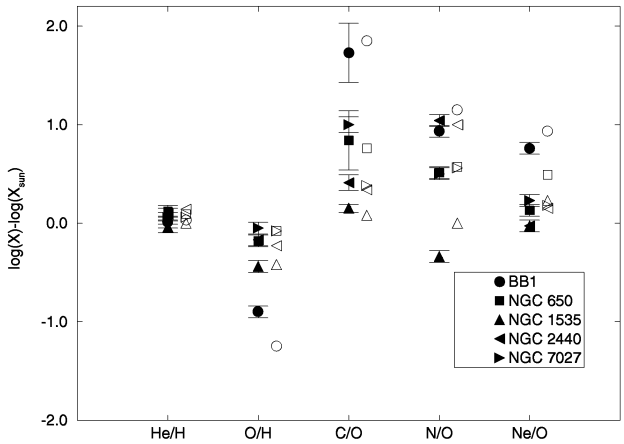

FIG. 1.—Five abundance ratios computed and normalized to their solar values (Grevesse & Anders 1989) are plotted logarithmically. Symbol shapes are used to designate each object (see legend). Filled symbols are our results, while open symbols refer to values found in the literature (see text for source references).

for the other ratios were taken from Perinotto (1991), which is a compilation of abundance averages from numerous sources.

Results displayed in Figure 1 indicate that all five objects are oxygen poor with respect to the Sun; in particular, BB 1—the one halo object in the group (*circles*)—is extremely oxygen poor, as anticipated from its classification as a halo object. Indeed, with the exception of NGC 7027, the relative O/H levels in these five PNs are roughly consistent with their Peimbert types. As we found with the first group of objects studied in Paper I, C/O and N/O ratios tend to be higher than the solar level here in all objects, with the possible exception of NGC 1535. Notice that, generally, our derived abundances agree closely with results from other sources (*open symbols*). For all but BB 1, Ne/O remains close to the solar value. The large Ne/O level for BB 1 has been seen before (cf. Peña et al. 1991; Henry 1990). A rather large discrepancy occurs between our value of C/O and that of Rola & Stasińska (1994) for NGC 7027, the source of which may be traced directly to the large correction [i.e., ξ(C/O)] we derived from the model by Péquignot et al. (1978). Rola & Stasińska obtained a value of 1.03 for C/O by assuming $C/O = C^{+2}/O^{+2}$, which is very close to our value of 1.18 obtained directly from the observed line strengths prior to applying the ξ correction. We note,

TABLE 4

DERIVED ABUNDANCES

	OBJECTS					
RATIO	BB 1	NGC 650	NGC 1535	NGC 2440	NGC 7027	Sun[a]
He/H.....	9.98(−2) ±0.15	0.13 ±0.15	0.09 ±0.15	0.12 ±0.15	0.11 ±0.15	9.80(−2)
O/H.....	1.07(−4) ±0.15	5.61(−4) ±0.15	3.12(−4) ±0.15	5.71(−4) ±0.15	5.08(−4) ±0.15	8.51(−4)
C/O	23.1 ±0.50	2.96 ±0.50	0.61 ±0.10	1.11 ±0.20	1.88 ±0.20	0.43
N/O.....	1.11 ±0.15	0.42 ±0.15	0.06 ±0.15	1.44 ±0.15	0.32 ±0.15	0.13
Ne/O.....	0.81 ±0.15	0.19 ±0.15	0.13 ±0.15	0.13 ±0.15	0.27 ±0.15	0.14
Type	Halo	I	II–III	I	II	...

[a] Grevesse & Anders 1989.

however, that while the model by Péquignot et al. (1978) is quite good overall, its predictions for C III] λ1909 and C IV λ1549 are too large by roughly a factor of 2. Thus, it may be that our value of ξ(C/O) is overcorrecting the ratio derived directly from the line strengths.

4. SUMMARY

This paper is the second in a series reporting on a study of carbon (and other) abundances in a well-defined sample of planetary nebulae representing a broad range in progenitor mass and metallicity. We take advantage of the Final Archive database—made available recently—that contains *IUE* spectra that have been reduced under a new system of algorithms. Thus, the reductions have been carried out consistently from object to object. We have measured collisionally excited emission lines of carbon and coupled these measurements to optical line strengths in the literature to determine abundance ratios of He/H, O/H, C/O, N/O, and Ne/O in five planetary nebulae: BB 1, NGC 650, NGC 1535, NGC 2440, and NGC 7027. The optical data were chosen carefully so as to overlap spatially as much as possible with the *IUE* observations.

These results continue to point to generally enhanced levels of C/O and N/O in planetary nebulae, with O/H levels consistent with object Peimbert types. Furthermore, our findings for these and other ratios are consistent with published values from earlier studies of the same objects. We postpone a thorough discussion of the implications of the abundance findings until we have completed the analysis of each of our sample objects.

This project is supported by NASA grant NAG 5-2389.

REFERENCES

Acker, A., Ochsenbein, F., Stenholm, B., Tylenda, R., Marcout, J., & Schohn, C. 1992, The Strasbourg/ESO Catalogue of Galactic Planetary Nebulae (Garching bei München: ESO)
Adam, J., & Köppen, J. 1985, A&A, 142, 461
Ferland, G. J. 1990, Ohio State Univ. Rep. 90-02
Grevesse, N., & Anders, E. 1989, in AIP Conf. Proc. 183, Cosmic Abundances of Matter, ed. C.J. Waddington (New York: AIP), 1
Gutiérrez-Moreno, A., Moreno, H., & Cortés, G. 1985, PASP, 97, 397
———. 1986, PASP, 98, 488
Henry, R. B. C. 1990, ApJ, 356, 229
Henry, R. B. C., Kwitter, K. B., & Howard, J. W. 1996, ApJ, 458, 215 (Paper I)
Hummer, D. G., & Storey, P. J. 1987, MNRAS, 224, 801
Kaler, J. B., Aller, L. H., Czyzak, S. J., & Epps, H. W. 1976, ApJS, 31, 163
Kaler, J. B., Shaw, R. A., & Kwitter, K. B. 1990, ApJ, 359, 392
Peimbert, M., & Torres-Peimbert, S. 1987, Rev. Mexicana Astron. Astrofiz., 14, 540
Peña, M., Torres-Peimbert, S., & Ruiz, M. T. 1991, PASP, 103, 865
Péquignot, D., Aldrovandi, S. M. V., & Stasińska, G. 1978, A&A, 63, 313
Perinotto, M. 1991, ApJS, 76, 687
Rola, C., & Stasińska, G. 1994, A&A, 282, 199
Savage, B. D., & Mathis, J. S. 1979, AR&A, 17, 73
Seaton, M. J. 1979, MNRAS, 187, 73
Shaw, R. A., & Kaler, J. B. 1982, ApJ, 261, 510
Shields, G. A., Aller, L. H., Keyes, C. D., & Czyzak, S. J. 1981, ApJ, 248, 569
Torres-Peimbert, S., & Peimbert, M. 1977, Rev. Mexicana Astron. Astrofiz., 2, 181
Torres-Peimbert, S., Rayo, J. F., & Peimbert, M. 1981, Rev. Mexicana Astron. Astrofiz., 6, 315